

Prompt fission γ -ray spectrum characteristics from $^{240}\text{Pu}(\text{sf})$ and $^{242}\text{Pu}(\text{sf})$

S. Oberstedt,^{1,*} A. Oberstedt,² A. Gatera,¹ A. Gök,¹ F.-J. Hambsch,¹ A. Moens,¹ G. Sibbens,¹
D. Vanleeuw,¹ and M. Vidali¹

¹European Commission, Joint Research Centre, Institute for Reference Materials and Measurements (IRMM),
Retieseweg 111, 2440 Geel, Belgium

²Fundamental Fysik, Chalmers Tekniska Högskola, 41296 Göteborg, Sweden

(Received 2 March 2016; published 4 May 2016)

In this paper we present first results for prompt fission γ -ray spectra (PFGS) characteristics from the spontaneous fission (sf) of ^{240}Pu and ^{242}Pu . For $^{242}\text{Pu}(\text{sf})$ we obtained, after proper unfolding of the detector response, an average energy per photon $\bar{\epsilon}_\gamma = (0.843 \pm 0.012)$ MeV, an average multiplicity $\bar{M}_\gamma = (6.72 \pm 0.07)$, and an average total γ -ray energy release per fission $\bar{E}_{\gamma,\text{tot}} = (5.66 \pm 0.06)$ MeV. The $^{240}\text{Pu}(\text{sf})$ emission spectrum was obtained by applying a so-called detector-response transformation function determined from the ^{242}Pu spectrum measured in exactly the same geometry. The results are an average energy per photon $\bar{\epsilon}_\gamma = (0.80 \pm 0.07)$ MeV, the average multiplicity $\bar{M}_\gamma = (8.2 \pm 0.4)$, and an average total γ -ray energy release per fission $\bar{E}_{\gamma,\text{tot}} = (6.6 \pm 0.5)$ MeV. The PFGS characteristics for $^{242}\text{Pu}(\text{sf})$ are in very good agreement with those from thermal-neutron-induced fission on ^{241}Pu and scales well with the corresponding prompt neutron multiplicity. Our results in the case of $^{240}\text{Pu}(\text{sf})$, although drawn from a limited number of events, show a significantly enhanced average multiplicity and average total energy, but may be understood from a different fragment yield distribution in $^{240}\text{Pu}(\text{sf})$ compared to that of $^{242}\text{Pu}(\text{sf})$.

DOI: [10.1103/PhysRevC.93.054603](https://doi.org/10.1103/PhysRevC.93.054603)

I. INTRODUCTION

In recent years the measurement of prompt fission γ -ray spectra (PFGS) has undergone a renaissance, motivated by requests for new precise values especially for γ -ray multiplicities and average photon energy release per fission in the thermal-neutron-induced fission of ^{235}U [1] and ^{239}Pu [2]. Improvements of nuclear data have now become possible due to advances in scintillator materials as used, e.g., in lanthanide halide detectors. They offer a superior combination of intrinsic peak efficiency, energy, and timing resolution, as already demonstrated in a number of recent experiments on $^{252}\text{Cf}(\text{sf})$ [3–5], $^{235}\text{U}(n_{\text{th}}, f)$ [4,6], and $^{241}\text{Pu}(n_{\text{th}}, f)$ [4,7].

Starting with $^{252}\text{Cf}(\text{sf})$, we are carrying out a measurement series on spontaneously fissioning actinides, and we present here first results on PFGS characteristics from the spontaneous fission of ^{240}Pu and ^{242}Pu . This campaign is motivated by the first parametrization to describe systematic trends of PFGS characteristics which was made by Valentine [8]. He introduced a somewhat arbitrary functional dependence of PFGS characteristics on the compound nucleus (CN) mass and atomic numbers as well as its prompt fission neutron multiplicity, accounting for the competition between the two deexcitation channels of prompt γ -ray and neutron emission. In this early work only spontaneous fission and thermal-neutron-induced fission were considered. Although the parameters obtained back then need an adjustment due to recently

published experimental results as shown in Refs. [9,10], more data are necessary in order to reduce the statistical uncertainties on the model parameters.

II. EXPERIMENT AND DATA TREATMENT

The prompt fission γ -ray measurements on ^{240}Pu and ^{242}Pu formed part of a series of experiments, which originally aimed at the precise measurement of their neutron-induced fission cross sections, in response to a high-priority request published through the OECD/NEA [11,12]. In the preparation of these measurements a precise determination of the spontaneous fission half-life of each isotope was achieved [13]. A prerequisite for such measurements is the availability of high-quality targets with high isotopic purity. The preparation of such targets was achieved at the European Commission, Joint Research Centre, Institute for Reference Materials and Measurements (EC-JRC IRMM) [14]. Detailed target specifications are listed in Table I.

Thin targets of ^{240}Pu and ^{242}Pu were placed back-to-back at the central cathode position inside a cylindrical twin Frisch-grid ionization chamber. The fission rates were 0.044/s and 0.54/s for ^{240}Pu and ^{242}Pu , respectively. The counting gas was methane at a pressure of 1.08×10^5 Pa at a flow-rate of about 90 ml/min, providing a detection efficiency for fission fragments close to 100% [13]. In coincidence with the fission fragments γ rays were measured with one cylindrical $\text{LaBr}_3:\text{Ce}$ scintillation detector (serial number A2987) of size $76.2 \text{ mm} \times 76.2 \text{ mm}$ (diameter \times length). The crystal was mounted onto a photomultiplier tube (PMT) from Hamamatsu (R10233-100-02) with a 89 mm diameter quartz window. A bias of +740 V was applied to the anode of the PMT.

The pulse height of the γ rays was calibrated with several standard radioactive sources with decay energies between 81 keV and 4.44 MeV, using ^{133}Ba (81–356 keV), ^{137}Cs

*Corresponding author: stephan.oberstedt@ec.europa.eu

TABLE I. Plutonium target characteristics as used in this work.

	^{240}Pu	^{242}Pu
Production method	Molecular plating	Molecular plating
Chemical composition (assumed)	$\text{Pu}(\text{OH})_4$	$\text{Pu}(\text{OH})_4$
Active diameter	29.95 (0.1%)	29.95 (0.1%)
Backing	Al	Al
Total mass (μg)	119.22 (0.4%)	859.54 (0.9%)
Total area density ($\mu\text{g}/\text{cm}^2$)	16.92 (0.4%)	122.0 (0.8%)
Mass (μg)	92.9 (0.4%)	671 (0.9%)
Area density ($\mu\text{g}/\text{cm}^2$)	13.19 (0.4%)	95.3 (0.8%)
α activity (MBq)	0.780 (0.4%)	0.0984 (0.3%)
Isotopic purity	99.8915(18)%	99.965 18(45)%

(662 keV), ^{60}Co (1173 keV, 1333 keV), ^{232}Th (583 keV, 2614 keV) and AmBe (decay of the first excited state in ^{12}C ; $E_\gamma = 4.44$ MeV). The low-energy threshold during the PFGS measurements was set to 100 keV.

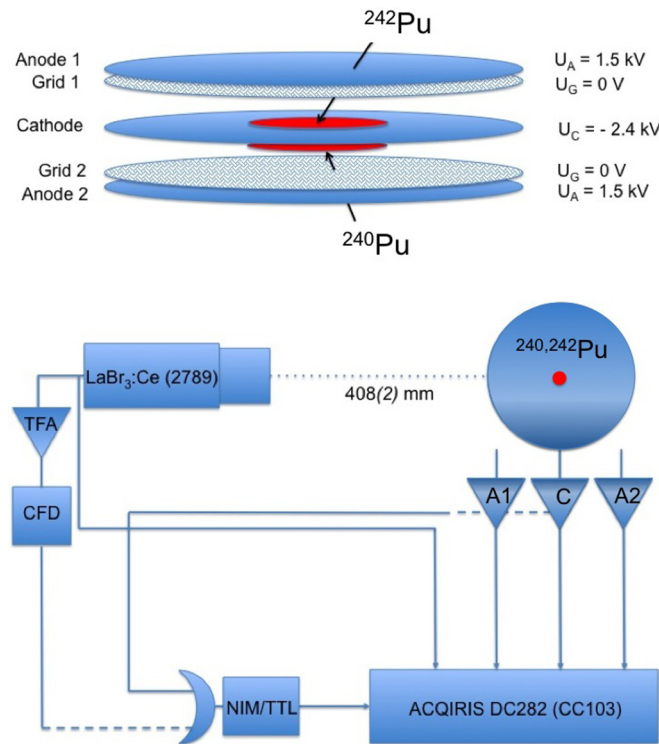


FIG. 1. (a) Setup used for the measurement of prompt fission γ -ray spectra from the spontaneous fission of ^{240}Pu and ^{242}Pu ; the active material was deposited on 0.25 mm thick Al backings, which were mounted back-to-back in the center of the cathode electrode of the ionization chamber. CH_4 (N50) at a flow rate of 90 ml/min was used as the counting gas. (b) Schematics of the electronics setup: signal traces were recorded with a digital acquisition system (10 bit resolution, 2 GHz sampling rate). The γ detector was a 76.2 mm \times 76.2 mm (diameter \times length) $\text{LaBr}_3:\text{Ce}$ detector, which was placed at a distance, relative to the end cap, of 408(2) mm from the fission targets (see text for more details).

The signal from the fission chamber's cathode is connected to preamplifier C, while anode 1 and anode 2 to preamplifiers A1 and A2 [15]. All signals were digitized with a multichannel ACQIRIS DC282 waveform-digitizer system, sampling with 10 bit and 2 Gs/s [16]. The acquisition system was triggered with the cathode. Due to the high α activity of the ^{240}Pu the current signal of preamplifier C was used. A sketch of the fission chamber, the target configuration, and the electronics is depicted in Fig. 1. Fission events were taken with and without coincident signals from the γ detector, as indicated by the dashed line in the figure.

Due to an unfavorable signal-to-noise ratio of the available cathode preamplifier in conjunction with the low number of bits, the achieved timing resolution was not better than 7.7 ns (FWHM). After a careful correction for walk, due to pulse-height-dependent timing of both cathode and γ -ray detector, a final timing resolution of 7 ns (FWHM) was achieved. This was still sufficient to discriminate prompt fission γ rays from photons created in other reactions by their time-of-flight relative to the instant of a fission event. With the γ -ray detector placed at a distance of 408(2) mm relative to the fission source all neutrons with energies below 6.5 MeV were discriminated.

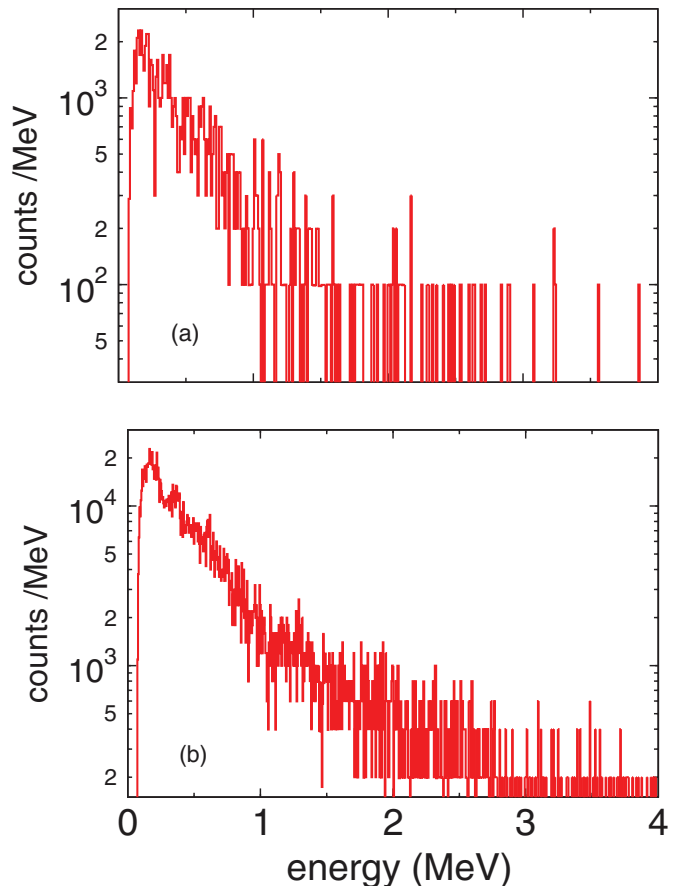


FIG. 2. Experimental prompt γ -ray spectra for (a) $^{240}\text{Pu}(\text{sf})$, depicted with 10 keV wide energy bins, and (b) $^{242}\text{Pu}(\text{sf})$ with 5 keV wide energy bins.

TABLE II. Number of fission events and number of γ rays detected in coincidence with a fission fragment.

	^{240}Pu	^{242}Pu
Fissions	69 642 (0.4%)	847 904 (0.1%)
γ rays (background corrected)	887.5 (3.4%)	8209.5 (1.1%)
Background γ rays (normalized)	1.5	17.6

Data were taken for 438 h. In total, 69 642 and 847 904 fission events were registered for ^{240}Pu and ^{242}Pu , respectively. The corresponding background-corrected numbers of prompt fission γ rays measured in coincidence with a fission fragment were 887.5 and 8209.5 (see Fig. 2 and Table II).

III. PROMPT FISSION γ -RAY CHARACTERISTICS FROM $^{242}\text{Pu}(\text{sf})$

To extract an emission spectrum from the measured one, the response function of the detector must be determined and unfolded. The usual procedure is to simulate, by means of Monte Carlo simulations, the response of the detector to monoenergetic γ rays accounting for the geometrical efficiency and the experimental setup. The resulting spectra are then adjusted to the measured spectrum (for details see Ref. [3]). Due to the limited number of events at energies above 3 MeV, an exponential was fitted to the experimental data above 1.8 MeV. When extracting the spectral characteristics the uncertainty of the coefficients of the exponential function were properly taken into account.

The resulting prompt fission γ -ray spectrum is depicted in Fig. 3 by the red line. For comparison we show the emission spectrum obtained previously for the neutron-induced fission of ^{242}Pu [7]. Both spectra agree very well with each other. The effect of the extra excitation energy in neutron-induced fission seems to be reflected in a surplus of photons at energies below 500 keV [Fig. 3(b)]. The spectral characteristics, integrated from $0.1 \leq E_\gamma \leq 7$ MeV, are summarized in Table III.

IV. PROMPT FISSION γ -RAY CHARACTERISTICS FROM $^{240}\text{Pu}(\text{sf})$

In the case of $^{242}\text{Pu}(\text{sf})$ we were able to perform the *standard* unfolding of the measured PFGS. This was not possible in the present study for $^{240}\text{Pu}(\text{sf})$ due to the poor counting statistics (cf. Table II). Instead we followed here a different approach, based upon the definition of a so-called *transformation function* as detailed in the following.

A. Definition of a transformation function

The method of applying a transformation function is motivated by the fact that we measured both spectral data from two samples in essentially the same position relative to the γ detector. Therefore, the response should be identical in both cases reported here. In addition, both measured spectra have to exhibit the same shape as we may observe in the case of $^{242}\text{Pu}(\text{sf})$ when compared to that from $^{242}\text{Pu}(n_{\text{th}}, f)$. Hence, we define a *transformation function* as the ratio between the

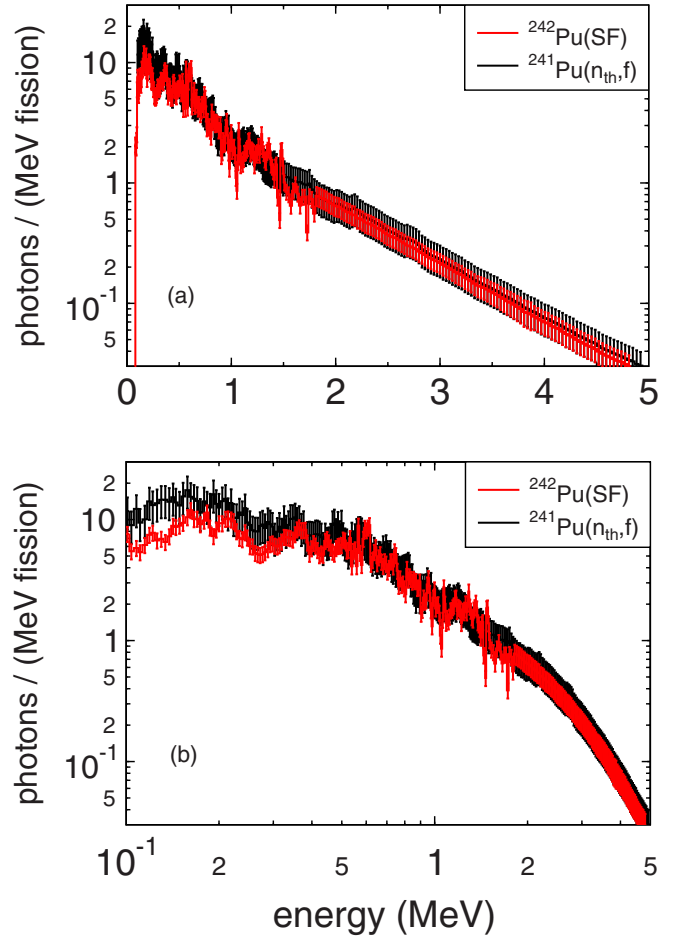


FIG. 3. (a) Prompt γ -ray spectrum for $^{242}\text{Pu}(\text{sf})$ in photons per MeV and per fission (red line); the corresponding spectrum for $^{241}\text{Pu}(n_{\text{th}}, f)$ [7] is shown for comparison (black line). Figure (b) shows the same data in logarithmic energy scale to emphasize the low-energy region.

emission spectrum and the measured spectrum, i.e.,

$$S_e(E_{\gamma,i}) = F_t(E_{\gamma,i}) \times S_m(E_{\gamma,i}) / N_{\text{fission}}. \quad (1)$$

Here, $S_e(E_{\gamma,i})$ denotes the emission spectrum, $S_m(E_{\gamma,i})$ the measured one, and $F_t(E_{\gamma,i})$ a transformation function. The

TABLE III. Average prompt fission γ -ray spectrum characteristics for the spontaneous fission of ^{240}Pu and ^{242}Pu from this work compared with corresponding results from thermal-neutron-induced fission on ^{241}Pu from Ref. [7] and from systematic trends established in Ref. [8].

$(^AX)_{\text{CN}}$	Δt (ns)	\overline{M}_γ (/fission)	$\overline{\epsilon}_\gamma$ (MeV)	$\overline{E}_{\gamma,\text{tot}}$ (MeV)	Ref.
^{242}Pu	± 10	6.72 ± 0.07	0.843 ± 0.012	5.66 ± 0.06	This work
^{242}Pu		6.5 ± 0.5	0.93 ± 0.07	6.05 ± 0.03	[8]
$^{242}\text{Pu}^*$	± 3	8.21 ± 0.09	0.78 ± 0.01	6.41 ± 0.06	[7]
^{240}Pu	± 10	8.2 ± 0.4	0.80 ± 0.07	6.6 ± 0.5	This work
^{240}Pu		6.4 ± 0.5	0.95 ± 0.07	6.07 ± 0.03	[8]

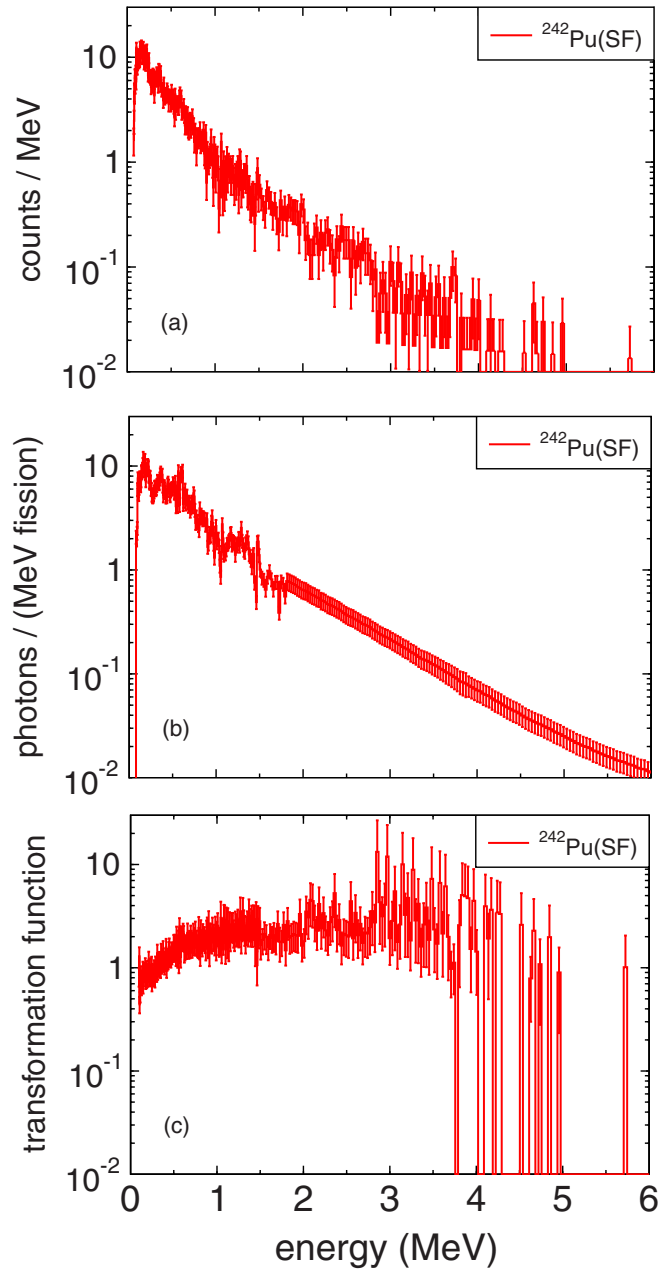


FIG. 4. (a) Measured PFGS spectra for $^{242}\text{Pu}(\text{sf})$. (b) Emission spectrum for $^{242}\text{Pu}(\text{sf})$. (c) Transformation function obtained from the ratio between the emission spectrum depicted in (b) and the measured spectrum shown in (a); see text for details.

latter was determined from the experiment on $^{242}\text{Pu}(\text{sf})$ and is shown in Fig. 4(c). The energies $E_{\gamma,i}$, for which $F_t(E_{\gamma,i})$ was calculated, correspond to the energies of the unfolded spectrum [Fig. 4(b)], to which the measured spectrum [Fig. 4(a)] was interpolated by using the Aitken-Neville method [17]. The uncertainties of the transformation function contain both the statistical ones from the measured spectrum and the uncertainties of the emission spectrum from the unfolding of the response function.

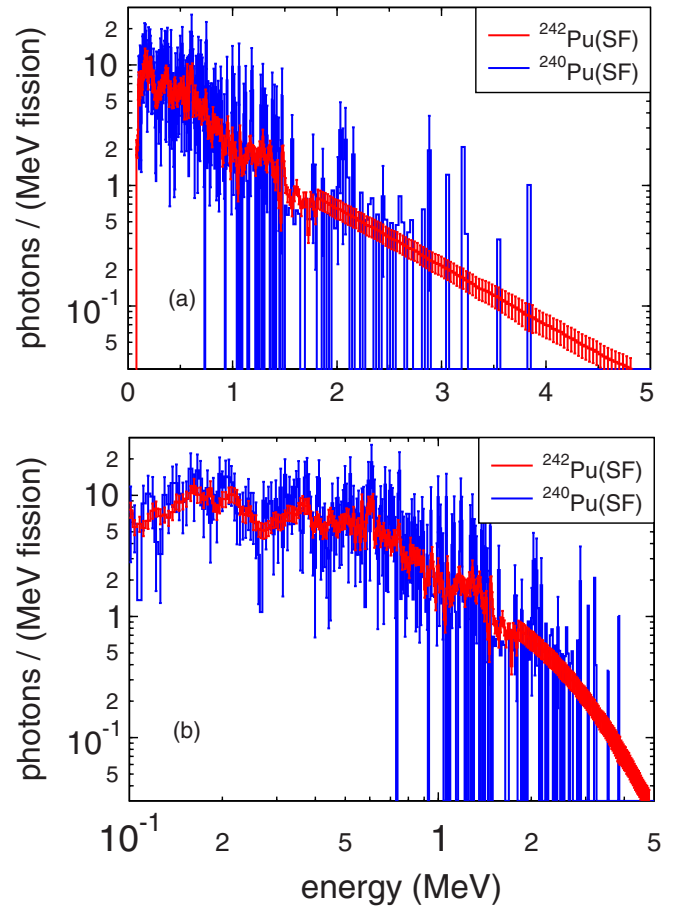


FIG. 5. (a) Prompt γ -ray spectra for $^{240}\text{Pu}(\text{sf})$ and $^{242}\text{Pu}(\text{sf})$ from this work depicted as full red and blue lines, respectively. Figure (b) shows the same data in logarithmic energy scale to emphasize the low-energy region.

B. Application of the transformation function

Prior to applying this transformation function to the measured prompt fission γ -ray spectrum from this work, new values and their uncertainties for matching energies were interpolated again. Finally, we obtained an emission spectrum as depicted as the full (blue) line in Fig. 5. The error bars include the statistical uncertainties from the measured spectrum and uncertainties in the transformation function [cf. Fig. 4(c)]. For comparison the PFGS for $^{242}\text{Pu}(\text{sf})$ is shown as a full (red) line. The spectral characteristics, integrated from $0.1 \leq E_\gamma \leq 4$ MeV, are summarized in Table III. In Figure 5(b) we show the same spectrum with a logarithmic energy scale to provide a better view of the low-energy part below 1 MeV. The excellent agreement between both emission spectra is obvious, which implies that also the measured spectra have the same shape indeed and, hence, one of the conditions for the meaningful application of a transformation function is fulfilled.

V. RESULTS AND DISCUSSION

Since we present here the first prompt fission γ -ray data from spontaneously fissioning ^{240}Pu and ^{242}Pu , we compare

TABLE IV. Absolute contributions to the total uncertainties of prompt fission γ -ray characteristics from our $^{242}\text{Pu}(\text{sf})$ measurement as given in Table III.

Type of uncertainty	\overline{M}_γ (/fission)	$\overline{\epsilon}_\gamma$ (MeV)	$\overline{E}_{\gamma,\text{tot}}$ (MeV)
Statistical (γ rays, fissions, number of simulations)	0.012	0.002	0.010
Systematic	0.058	0.010	0.05 %
(i) Simulation (setup, cross sections)	55.1 %	55.1 %	55.0 %
(ii) Energy calibration	—	0.2 %	0.3 %
(iii) Fitting detector response	44.9 %	44.8 %	44.7 %

our results in Table III with spectral characteristics drawn from the above-mentioned trend established by Valentine [8]. A detailed decomposition of the uncertainties is presented in Tables IV and V.

In the case of $^{242}\text{Pu}(\text{sf})$ the agreement is very reasonable, taking into account that the trend is based on the few experimental data available back then. The mean energy per photon, ϵ_γ , is close to 0.8 MeV. From our previous measurements we have evidence that the average energy per photon shows only weak dependence on the compound system and even on the incident neutron energy. That the multiplicity is somewhat higher is in line with our findings in $^{252}\text{Cf}(\text{sf})$ [3–5], $^{235}\text{U}(n_{\text{th}}, f)$ [4,6], and $^{241}\text{Pu}(n_{\text{th}}, f)$ [4,7]. This is understandable when remembering that the low-energy threshold in our measurements is in most cases lower than in measurements conducted in the past. The different average multiplicity, \overline{M}_γ , observed between spontaneous and neutron-induced fission of ^{242}Pu scales well with the average total prompt neutron multiplicity for both fissioning systems, $\overline{\nu}_{\text{sf}} = 2.134(6)$ and $\overline{\nu}_{\text{th}} = 2.946(6)$ [18]. The influence of the different widths of the prompt time window, Δt (cf. Table III), may be neglected, because $\Delta t \geq 3.36\sigma_t$ in both cases.

For $^{240}\text{Pu}(\text{sf})$, \overline{M}_γ appears at first sight to be pretty high, definitely when compared with the predictions drawn from Valentine's trend. The differences may be regarded as significant despite the much larger uncertainty. However, our value for the average energy per photon, $\epsilon_\gamma = 0.8$ MeV, is well in agreement with all our other results, providing us with confidence in our new PFGS data for $^{240}\text{Pu}(\text{sf})$ as well as in the underlying data analysis.

Systematic measurements of pre-neutron mass distributions from different spontaneously fissioning plutonium isotopes have revealed significant changes in fission fragment yield distribution as a function of neutron number of the compound nucleus [19]. Starting from ^{238}Pu , the maximum yield of heavy fragments, A_h , is around 142 u. This position moves down to $A_h \approx 135$ u for ^{242}Pu , i.e., increasing the fraction

of less-deformed fragments being close to the doubly magic isotope ^{132}Sn . One might, therefore, argue that for $^{240}\text{Pu}(\text{sf})$ the dominant fraction of deformed fragments leads to an enhanced multiplicity due to higher level densities manifesting in a higher \overline{M}_γ .

However, one must not forget that for both spontaneously fissioning isotopes $\overline{\nu}_{\text{sf}}$ is essentially the same with $\delta\overline{\nu}_{\text{sf}}(^{240}\text{Pu}, ^{242}\text{Pu}) < 0.4\%$ [18]. In Ref. [19] we find that the average total kinetic energy, \overline{E}_k , is lower for $^{240}\text{Pu}(\text{sf})$ by almost 2 MeV. This small amount of more excitation energy, depending on the Q value of the reaction, does not seem to lead to an enhanced average neutron multiplicity, but may account for the excess observed for \overline{M}_γ . To determine whether the arguments brought forward here are contradictory or a hint that excitation energy in fission available at scission and in the fragments reflect differently on $\overline{\nu}$ and \overline{M}_γ requires the study of many more spontaneous fission systems.

VI. CONCLUSION

PFGS characteristics from the spontaneous fission of ^{240}Pu and of ^{242}Pu were measured for the first time with reasonable statistical accuracy. This was possible for ^{240}Pu by applying a transformation function to the measured spectrum in order to deduce the emission spectrum from a measured spectrum instead of a proper unfolding procedure by a response function. The transformation function was obtained from $^{242}\text{Pu}(\text{sf})$ measured with sufficient statistics under exactly the same conditions. This procedure seems to work well as long as reference spectra exist that have a very similar shape, which is the case here. Hence, this technique should be considered as an alternative, if recorded spectra are obtained from a low number of events. Moreover, a mathematical justification for this procedure is given in Ref. [20], where the transformation function $F_t(E_{\gamma,i})$ used in Eq. (1) is explained as a zero-order approximation of the correct response matrix.

 TABLE V. Same as Table IV, but for $^{240}\text{Pu}(\text{sf})$.

Type of uncertainty	\overline{M}_γ (/fission)	$\overline{\epsilon}_\gamma$ (MeV)	$\overline{E}_{\gamma,\text{tot}}$ (MeV)
Statistical (γ rays, number of fissions)	0.31	0.06	0.42
Statistical [total uncertainty from $F_t(E_{\gamma,i})$; see Sec. IV A for details]	0.17	0.04	0.29
Total uncertainty (cf. Table IV)	0.35	0.07	0.51

The results presented in this work fit well into the trend established by Valentine [8] and recently revised in Refs. [9,10]. They may be regarded as the first step to enlarging the data base from which new systematic trends as a function of incident neutron energy are established. The latter will be addressed in a forthcoming paper.

The significantly enhanced average multiplicity in case of $^{240}\text{Pu}(\text{sf})$ points to a possible correlation of prompt γ -ray emission with the distinct shape of the fission fragment distribution. To fully understand the underlying physics, more data are needed. Exchange with theoreticians is highly encouraged. In particular, PFGS measurements on $^{244}\text{Pu}(\text{sf})$

and different spontaneously fissioning curium isotopes are recommended. For the latter also measurements of pre-neutron fragment distributions $Y(A, E_k)$ will be indispensable. A PFGS measurement of the reaction $^{239}\text{Pu}(n_{\text{th}}, f)$ for comparison with $^{240}\text{Pu}(\text{sf})$ in analogy to the presented ^{242}Pu case is the subject of an ongoing campaign.

ACKNOWLEDGMENTS

The authors are indebted to P. Talou (LANL) and N. Carjan (IFINN-HH) for valuable discussions and their interest in this work. The European Commission is gratefully acknowledged for providing Ph.D. fellowship program support to A.G.

-
- [1] Nuclear Data High Priority Request List of the NEA (Req. ID: H.4), www.oecd-nea.org/dbdata/hprl/hprlview.pl?ID=422.
- [2] Nuclear Data High Priority Request List of the NEA (Req. ID: H.3), www.oecd-nea.org/dbdata/hprl/hprlview.pl?ID=421.
- [3] R. Billnert, F.-J. Hamsch, A. Oberstedt, and S. Oberstedt, *Phys. Rev. C* **87**, 024601 (2013).
- [4] R. Billnert, T. Belgya, T. Brys, W. Geerts, C. Guerrero, F.-J. Hamsch, Z. Kis, A. Oberstedt, S. Oberstedt, L. Szentmiklosi, K. Takács, and M. Vidali, *Phys. Procedia* **59**, 17 (2014).
- [5] A. Oberstedt, R. Billnert, F.-J. Hamsch, and S. Oberstedt, *Phys. Rev. C* **92**, 014618 (2015).
- [6] A. Oberstedt, T. Belgya, R. Billnert, R. Borcea, T. Brys, W. Geerts, A. Göök, F.-J. Hamsch, Z. Kis, T. Martinez, S. Oberstedt, L. Szentmiklosi, K. Takács, and M. Vidali, *Phys. Rev. C* **87**, 051602(R) (2013).
- [7] S. Oberstedt, R. Billnert, T. Belgya, T. Brys, W. Geerts, C. Guerrero, F.-J. Hamsch, Z. Kis, A. Moens, A. Oberstedt, G. Sibbens, L. Szentmiklosi, D. Vanleeuw, and M. Vidali, *Phys. Rev. C* **90**, 024618 (2014).
- [8] T. E. Valentine, *Ann. Nucl. Energy* **28**, 191 (2001).
- [9] A. Oberstedt, R. Billnert, and S. Oberstedt, in *Proceedings of NEMEA-7, The 7th Workshop on Nuclear Measurements, Evaluations and Applications, November 5–8*, (Geel, Belgium, 2013), OECD Nuclear Science NEA/NSC/DOC-2014-13, 2014, p. 199.
- [10] A. Oberstedt, R. Billnert, and S. Oberstedt (unpublished).
- [11] Nuclear Data High Priority Request List of the NEA (Req. ID: H.37), www.oecd-nea.org/dbdata/hprl/hprlview.pl?ID=457.
- [12] Nuclear Data High Priority Request List of the NEA (Req. ID: H.39), www.oecd-nea.org/dbdata/hprl/hprlview.pl?ID=457.
- [13] P. Salvador-Castineira, T. Brys, R. Eykens, F. J. Hamsch, A. Moens, S. Oberstedt, G. Sibbens, D. Vanleeuw, M. Vidali, and C. Pretel, *Phys. Rev. C* **88**, 064611 (2013).
- [14] G. Sibbens, A. Moens, R. Eykens, D. Vanleeuw, F. Kehoe, H. Kühn, R. Jakopic, S. Richter, A. Plompen, and Y. Aregbe, *J. Radioanal. Nucl. Chem.* **299**, 1093 (2014).
- [15] www.mesytec.com/datasheets/MPR-1.pdf.
- [16] <http://www.keysight.com/en/pd-1184897-pn-U1065A/acqiris-10-bit-high-speed-cpci-digitizers?&cc=BE&lc=dut>.
- [17] I. N. Bronstein, K. A. Semendjajew, G. Musiol, and H. Mühlig, *Taschenbuch der Mathematik mit Multiplattform-CD-ROM*, 5th ed. (Verlag Harri Deutsch, Frankfurt am Main, 2000).
- [18] F. Gönnewein, in *The Nuclear Fission Process*, edited by C. Wagemans (CRC, Boca Raton, FL, 1991), Chap. 11, p. 514.
- [19] L. Demattè, C. Wagemans, R. Barthelemy, P. D'Hondt, and A. Deruytter, *Nucl. Phys. A* **617**, 331 (1997).
- [20] R. Gold, An Iterative Unfolding Method for Response Matrices, Argonne National Laboratory, ANL-6984, 1964 (unpublished).